DOI: 10.30511/pcdp.2024.718536 - ISSN: 3060-8376 - Vol 1(1), 2024

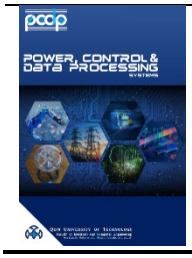

POWER, CONTROL AND DATA PROCESSING SYSTEMS

Available Online at: https://pcdp.qut.ac.ir/

Optimal Energy Management of Water-Energy Nexus in Multi-Carrier Systems Integrated with Renewable Sources

ARTICLE INFO

Article Type
Original Research

Authors
Mahdieh Monemi Bidgoli[1, *]

[1] Independent Researcher
m.monemi@hafez.shirazu.ac.ir

*** Correspondence***
Address: Independent Researcher
Phone: -
Fax: -
m.monemi.b@gmail.com

Article History
Received: November 07, 2024
Accepted: November 26, 2024
ePublished: December 01, 2024

ABSTRACT

This paper proposes a plenary structure of an energy hub system to combine electrical, thermal, cooling, and water infrastructures to promote modern distribution systems and increase flexibility and efficiency. The LSTM neural network predicts electrical loads with controlling variables such as air temperature, wind speed, humidity, holidays, and weekends. It is assumed that the system operator likes to use groundwater sources better. However, climate change, land subsidence, droughts, destruction of glaciers and lakes, dust storms, and inadequate water and food sources for future generations are the main challenges of unsustainable use of groundwater sources. A multi-objective optimization is proposed to simultaneously keep down the total operating costs and use of groundwater sources in the system. Renewable energy resources, electric vehicles, responsive electrical and thermal load programs, and energy storage systems have been developed to increase flexibility in the proposed system and are tried out in a standard case study. The simulation results show that the proposed approach reduces groundwater extraction by 26.88%.

Keywords: Energy hubs, Electrical load prediction, Renewable energy sources, Water desalination, Multi objective optimization.

1 Introduction

Due to the growth in electricity and thermal energy consumption and the need for reliable, safe, and frugal, energy hub systems effectively provide services to end-users with minimal environmental impact [1]. An energy hub system is a system that controls various energy carriers such as electricity, natural gas, cooling, heating, and water in an integrated manner [2,3]. Increased flexibility, efficiency, effectiveness, and reduced greenhouse gas emissions have made the integrated planning of energy hub systems a topic of specific interest [4,5].

Multiple papers have been conducted on the optimal performance of energy hub systems. The potential relation between renewable energy sources (RESs) and the load demand of an energy hub system has been in [6,9]. A combined stochastic method with information gap decision theory has been proposed in [7] to demonstrate the impact of electric vehicles (EVs) on the performance of an energy hub system. Mid-term energy management of multi-carrier networks considering the intermittent behavior of RESs has been investigated in [8] using robust optimization. The [11], has proposed a novel energy hub system approach for estimating the electricity consumption of EVs. Also, the authors in [12] have evaluated the efficiency of various types of EVs with different penetration rates on the management skills of an energy hub system. In several studies, the combination of many energy types such as heat, cooling, electricity, and water in an energy hub system has been proposed [10-13]. However, the lack of consideration for the role of the cooling storage system converter in [13], the lack of EVs in [10], the lack of consideration for demand-side management in [11], the lack of consideration for the thermal storage system in [12], and the limitation of water energy in [14] have created a research gap to provide a comprehensive modern energy hub system, which this paper attempts to address.

Industrial desalination units usually use saline waters to supply, the necessary freshwater for their customers. As the energy consumption of these units for water desalination is very high, in this study, we have assumed that the system operator prefers to use groundwater sources. However, climate change, drought, dust storms, land subsidence, wetland and lake degradation, and insufficient water and food for future generations are the main issues with the intolerable use of groundwater sources. Therefore, we propose a multi-objective optimization to simultaneously minimize the total operating costs and the use of groundwater sources in the proposed system.

The main contributions of this paper can be summarized as follows:

- The first objective of this paper is to provide a comprehensive structure of the energy hub system that integrates the electricity, heating, cooling, and water processes.
- The second objective is to provide a multi-objective decision-making difficulty to reduce the system's operating costs and protect groundwater sources.
- Ultimately, the proposed optimal energy management of water-energy nexus in multi-carrier systems is integrated with renewable sources. The configuration of the proposed energy hub system is shown in Fig.1.

This article is organized as follows: section 2 describes the mathematical formulations of the proposed method. section 3 presents multi-objective decision-making. A simulation analysis of the suggested model is developed in section 4. Finally, in section 5 conclusions with future work are given.

2 Mathematical formulation of the proposed method

The objective functions and physical constraints of sources are described in this section. The operating cost of the proposed system is shown in Eqs. (1) to (8) [19,20]. Equation (1) represents the day-ahead operating cost of the system, which includes the cost of electricity trading with the main network, the operating cost of the CHP unit, the operating cost of the boiler, the costs of electrical and thermal demand response (DR), and the cost of greenhouse gas emissions. The volume of freshwater extracted from groundwater sources is another objective function shown in Eq. (8). In this equation, EW^{water} presents the volume of groundwater extracted within the planning horizon.

$$\text{Minimize} Cost = Cost^{grid} + Cost^{CHP} + Cost^{boiler} + Cost^{EDR} + Cost^{HDR} + Cost^{emission} \quad (1)$$

$$Cost^{grid} = \sum_t \sum_s \rho_s P_t^g \pi_t^e \quad (2)$$

$$Cost^{CHP} = \sum_t G_t^{chp} \lambda_t^g \quad (3)$$

$$Cost^{boiler} = \sum_t G_t^{boiler} \lambda_t^g \quad (4)$$

$$Cost^{EDR} = \sum_t (CR_{dr}^{e,down} PD_t^{e,down} + CR_{dr}^{e,up} PD_t^{e,up}) \quad (5)$$

$$Cost^{HDR} = \sum_t (CR_{dr}^{h,down} PD_t^{h,down} + CR_{dr}^{h,up} PD_t^{h,up}) \quad (6)$$

$$Cost^{emission} = \sum_t C^{e,co_2} (P_t^g U^{grid,co_2} + (P_t^{e,chp} + P_t^{h,chp}) U^{chp,co_2} + H_t^{boiler} U^{boiler,co_2}) \quad (7)$$

$$\text{Minimize} EW^{water} = \sum_t Q_t^{w,w} \quad (8)$$

Energy storage systems (ESSs) play a vital role in energy hub systems and make the system more pliable. Charging /discharging energy determines how energy is recognized and adjusted in different periods. When the energy price is low and high, charging and discharging occur, respectively. In a surplus state, energy is stored in the ESSs, and energy is released in case of energy shortage. Equations (9) to (14) show the physical constraints of the ESSs. Equation (9) shows the electrical ESS's state of charge (SoC). The upper and lower bounds for the SoC are provided in Eq. (10). The constraints for the charging/discharging power are modeled by Eqs. (11) and (12), respectively. Equation (13) determines the mode of charging or discharge. Finally, Eq. (14) explains that the initial and final energies in the ESS must be equal [40]. Similarly,

equations for the HSS and ISC energy storage systems have been considered [21,22].

$$ES_t^{es} = ES_{t-1}^{es} + (P_t^{es,ch}\eta^{es,ch}) - (\frac{P_t^{es,disch}}{\eta^{es,disch}}) \quad (9)$$

$$E_{min}^{es_t^{es}} \quad (10)$$

$$0 \le P_t^{es,ch} \le P_{max}^{es,ch_t^{es,ch}} \quad (11)$$

$$0 \le P_t^{es,disch} \le P_{max}^{es,disch_t^{es,disch}} \quad (12)$$

$$0 \le EE_t^{es,ch} + EE_t^{es,disch} \le 1 \quad (13)$$

$$ES_0^{es} = ES_{24}^{es} \quad (14)$$

In the proposed system, RESs in the form of wind turbine (WT) and photovoltaic (PV) units have been considered. The power generated by the PV and WT units in scenario s and time t is shown in Eqs. (15) and (16), respectively [23]. In this study, Weibull and Beta probability distribution functions are used to present the fluctuations in the production of wind and solar units, which are commonly used in reliable studies [24]. Additionally, mixed-integer linear programming (MILP) has been used to reduce scenarios with low probability and decrease the computation speed. Reference [24] discusses scenario reduction methods in detail.

$$0 \le PD_t^{e,up} \le MRL^{e,up}L_t^{el}II_t^{e,up} \quad (17)$$

$$0 \le PD_t^{e,down} \le MRL^{e,down}L_t^{el}II_t^{e,down} \quad (18)$$

$$\sum_t PD_t^{e,up} = \sum_t PD_t^{e,down} \quad (19)$$

$$0 \le II_t^{e,up} + II_t^{e,down} \le 1 \quad (20)$$

The SoC of EVs is shown by Eq. (21). Equation (22) limits the SoC of the EVs between minimum and maximum values. The power consumption in their move mode is calculated using Eq. (23). Equations (24) and (25) show the charging and discharging ranges of each EV. Finally, the operation of EVs is determined by Eq. (26) [26].

$$SOC_{t,v}^{pev} = SOC_{t-1,v}^{pev} + (P_{t,v}^{pev,ch}\eta_v^{pev,ch}) - (\frac{P_{t,v}^{pev,disch}}{\eta_v^{pev,disch}}) - P_{t,v}^{pev,tr} \quad (21)$$

$$SOC_{min}^{pev_{t,v}^{pev}} \quad (22)$$

$$P_{t,v}^{pev,tr} = \Delta D_{t,v}^{pev} \times \eta_v^{pev} \quad (23)$$

$$0 \le P_{t,v}^{pev,ch} \le P_{max}^{pev,ch_{t,v}^{pev,ch}} \quad (24)$$

$$0 \le P_t^{pev,disch} \le P_{max}^{pev,disch_{t,v}^{pev,disch}} \quad (25)$$

$$0 \le PP_{t,v}^{pev,ch} + PP_{t,v}^{pev,disvh} \le 1 \quad (26)$$

The main objective of the energy hub system is to support the required electrical, thermal, and cooling energy to the consumers. For this goal, it must keep thermal, electrical, and cooling balances. Equations (27) to (45) are considered for this purpose. The heat generated by the boiler unit is defined by Eq. (30). Equations (31) and (33) explain the electrical power and thermal energy created by the CHP, respectively. The input gas to the CHP and the boiler is limited by Eqs. (33) and (34). Electricity purchases from the upstream grid and the thermal pipes are expressed by Eqs. (35) and (36), respectively. The charging power of the ISC is described by Eq. (37), and its input power is limited by Eq. (38). The output of the electric chiller is shown by Eq. (39), and (40) limits its input power. The output of the absorption chiller is also shown by Eq. (41), and its input heat is limited by Eq. (42). The heat produced by the boiler is also shown by Eq. (43), and finally, the input gas from the gas network is limited by Eqs. (44) and (45) [27].

$$P_t^g + \sum_s(P_{t,s}^{pv} + P_{t,s}^{wt}) + P_t^{e,chp} + PD_t^{e,down} + P_t^{es,disch} + \sum_v P_{t,v}^{pev,disch} = L_t^{el} + PD_t^{e,up} + P_t^{es,ch} + \sum_v P_{t,v}^{pev,ch} + P_t^{isc} + P_t^{ec} + P_t^{water,w} \quad (27)$$

$$P_t^{h,chp} + H_t^{boiler} + PD_t^{h,down} + P_t^{hs,disch} = L_t^{hl} + PD_t^{h,up} + P_t^{hs,ch} + H_t^{ac} \quad (28)$$

$$C_t^{ec} + C_t^{ac} + P_t^{cs,disch} = L_t^{cl} \quad (29)$$

$$H_t^{boiler} = G_t^{boiler}LHV\eta^{boiler} \quad (30)$$

$$P_t^{e,chp} = G_t^{chp}LHV\eta^{e,chp} \quad (31)$$

$$P_t^{h,chp} = G_t^{chp}LHV\eta^{h,chp} \quad (32)$$

$$0 \le G_t^{chp} \le G_{max}^{chp} \quad (33)$$

$$0 \le G_t^{boiler} \le G_t^{boiler} \quad (34)$$

$$-L_{max}^{grid_{t\ max}^{ggrid}} \quad (35)$$

$$0 \le P_t^{h,chp} + H_t^{boiler} + P_t^{hs,disch} - P_t^{hs,ch} - H_t^{ac} \le P_{max}^{h} \quad (36)$$

$$P_t^{cs,ch} = P_t^{isc}COP^{isc} \quad (37)$$

$$0 \le P_t^{isc} \le P_{max}^{isc} \quad (38)$$

$$C_t^{ec} = P_t^{ec}COP^{ec} \quad (39)$$

$$0 \le P_t^{ec} \le P_{max}^{ec} \quad (40)$$

$$C_t^{ac} = H_t^{ac}COP^{ac} \quad (41)$$

$$0 \le H_t^{ac} \le H_{max}^{ac} \quad (42)$$

$$0 \le H_t^{boiler} \le H_{max}^{boiler} \quad (43)$$

$$P_t^{gas} = G_t^{boiler} + G_t^{chp} \quad (44)$$

$$0 \le P_t^{gas} \le p_{max}^{gas} \quad (45)$$

For the water system, the power consumption of water pumping from the well is a function of flow and head, which is specified by Eqs. (46) and (47) [20]. Using desalination is another way to meet the system's water demand. The power consumption of water desalination is defined by Eq. (48), and the water produced by the desalination unit is limited by Eq. (49). The physical constraints of the water storage system are shown in Eqs. (50) to (54). Equation (50) describes the water level in the water storage system, and Eq. (51) relates the allowable water levels. The amount of water charging and discharging is limited in Eqs. (52) and (53). Equation (54) vouchs that the water storage system can only work in one of the charging or discharging modes at a time. Finally, the water balance and the electrical power used by the water section are shown in Eqs. (55) and (56), respectively [20].

$$P_t^{pw,w} = Q_t^{w,w}LL^{w,w}\frac{g^w\rho^w}{\eta^{p,w}(3.6\times10^6)} \quad (46)$$

$$P_t^{ps,w} = Q_t^{w,ch}(L_t^{s,w} + L_{t-1}^{s,w} + LL^{g,w})\frac{g^w\rho^w}{2\eta^{p,w}(3.6\times10^6)} \quad (47)$$

$$P_t^{d,w} = \eta^{d,w}Q_t^{d,w} \quad (48)$$

$$0 \le Q_t^{d,w} \le Q_{max}^{d,w} \quad (49)$$

$$L_t^{s,w} = L_{t-1}^{s,w} + (\frac{Q_t^{w,ch}}{A^{s,w}}) - (\frac{Q_t^{w,disch}}{A^{s,w}}) \quad (50)$$

$$0 \le L_t^{s,w} \le L_{max}^{s,w} \quad (51)$$

$$0 \le Q_t^{w,ch} \le Q_{max}^{w,ch_t^{w,ch}} \quad (52)$$

$$0 \le Q_t^{w,disch} \le Q_{max}^{w,disch} {}^{w,disch}_{t} \quad (53)$$

$$0 \le WW_t^{w,ch} + WW_t^{w,disch} \le 1 \quad (54)$$

$$Q_t^{w,w} + Q_t^{d,w} + Q_t^{w,disch} = Q_t^{w,ch} + L_t^{wl} \quad (55)$$

$$P_t^{water,w} = P_t^{d,w} + P_t^{pw,w} + P_t^{ps,w} \quad (56)$$

In this paper, an hourly electric load forecasting process using the long-short term memory (LSTM) neural network has been proposed. The forecasted load is related to the total electrical load of Panama country. The proposed forecasting model consists of two main stages. The first stage is to prepare the entire dataset, including input and output features, for the deep learning process through the pre-processing stage, which is associated with the data mining process. The second stage trains the LSTM neural network to obtain a correct model that can map the nonlinear relationship between the system features. To reduce the data size, each consumer is presented with a so-called load curve. These curves are obtained by averaging the daily load shapes for different hours of each consumer, and these curves will be evaluated. Since electric load forecasting topics are time series, the data structure must be transformed into a time series format for neural network training. Economic and climatic elements such as temperature, humidity, wind speed, precipitation, and time affect the load consumption, which we have used in this study to forecast the daily load curve [20] and [28].

3 Multi-objective decision making

The study investigates the optimal performance of the energy hub system from both the ecosystem and economic views. A multi-objective decision-making framework is used to select the best design. A normalized weighted sum method is proposed to convert the original multi-objective problem into a single-objective problem. This method has the advantage of recognizing a single optimal solution. The objective function model for the optimization operations is defined according to Eq. (57), where F^{Ideal} and F^{Nadir} present the best and worst solutions for each objective, respectively. Fig. 2 illustrates the simulation steps.

$$Min\left(w_1^g \frac{F_1}{F_1^{Nadir} - F_1^{Ideal}} + w_2^g \frac{F_2}{F_2^{Nadir} - F_2^{Ideal}}\right)$$
$$\sum w_i^g = 1, w_i^j \in (0,1) \quad (57)$$

4 Simulation Analysis

The daily electrical load profile in three Panama cities has been considered hourly, from 2015 to 2020. Meteorological features (such as temperature, humidity, wind speed, and precipitation) and holidays (Saturdays, Sundays, and national holidays) are applied as exogenous variables in the proposed models. The average daily temperature and humidity are not fixed and have a significant range, indicating different seasonal and meteorological characteristics in Panama Country. Among the selected elements, the temperature has the highest correlation with the load, although the load has different correlation levels in summer and winter [31]. The upper limit of the hourly power swapping with the upstream network is assumed to be 500 kw, and the system under study includes ten EVs with parameters taken from reference [26]. The specs of the cooling, electrical, and thermal converters are given in Table 1, and the characteristics of the CHP unit and the boiler are shown in Table 2 [20].

The study uses 80% of the daily data from the 5 years as the training data to fit the models and 20% as the test data to figure out the model performance. Figure 3 shows a representation of the predicted electrical power. The correlation factor of the exogenous variables shows that the study did not identify any strong (greater than 0.8) or mild (greater than 0.6) correlations. The planning horizon of the system is deemed to be 24 hours, and for optimal and secure system operation, the data for each hour is averaged. The study uses Python statistical software for load data management and analysis and the GAMS software for investigating the proposed optimization model method, and two case studies are examined to appraise the simulation results.

Case study 1; This case moots the energy hub system with an objective function that puts only the operating costs and does not consider the cost of water supply.

Case study 2; This case considers the proposed energy hub system cum a multi-objective function that consists of both the operating costs and the cost of water supply.

The system optimizes the operating costs and groundwater sources to gain a balance between ecosystem and operational costs. The main findings show as from the simulation results (see Figs. 4 to 11), that the electricity consumption by the water network increased in the proposed model (case study 2) compared to case study 1. In case study 2, the system prefers to increase the availability of the desalination unit to reduce the extraction from groundwater sources. Also, the simulation results show that the proposed energy hub system shifts its load to off-peak hours to reduce operating costs. The PEVs and ESSs are charged during off-peak hours and discharged during peak hours to take the upper hand in the lower electricity prices. Similarly, thermal energy storage is also charged during off-peak hours and discharged during peak hours to reduce the overall system costs. The water balance shows that in case study 1, the system extracts the maximum acceptable water from groundwater, while the proposed model reduces the extraction to support the groundwater sources by 26.88%. The thermal balance shows that the CHP unit works at maximum capacity most of the time because of its low production cost, and the excess heat is used for cooling. Ultimately, the cooling balance shows that the electric chiller is essential to meet the cooling demands of the system. Overall results, the proposed multi-objective model in case study 2 illustrates the ability to balance the ecosystem and operational costs by optimizing the energy hub system design and operation.

5 Conclusion

This article willing a multi-objective decision-making framework for optimal energy management in modern energy hub systems using predicted electrical loads and considering economic and environmental specifications. The proposed model targets to keep safe groundwater sources and supplies a major portion of the required freshwater through a desalination unit. The proposed model improves the total water cost of the system and stops environmental risks such as deterioration of water quality, well depletion, and land subsidence. Additionally, the system's thermal and electrical demand management is combined to reduce its operating cost. Moreover, electrical, thermal, water, and ice storage systems increase the system's energy flexibility to manage the alternative behavior of RESs. The optimization results show that the proposed method reduces groundwater extraction by 26.88%. In future studies, we intend to test the proposed model on several modern energy hub systems and model the coordination between the systems using game theory.

Disclosure of Potential Conflicts of Interest

The Authors declare that there is no conflict of interest

Reference

[1] R. Carli, G. Cavone, T. Pippia, B. De Schutter, and M. Dotoli, "Robust optimal control for demand side management of multi-carrier microgrids," IEEE Transactions on Automation Science and Engineering, vol. 19, no. 3, pp. 1338-1351, 2022.

[2] S. M. Ali and A. Acquaye, "An examination of Water-Energy-Food nexus: From theory to application," Renewable and Sustainable Energy Reviews, vol. 202, p. 114669, 2024.

[3] M. Sajna et al., "Integrated seawater hub: A nexus of sustainable water, energy, and resource generation," Desalination, vol. 571, p. 117065, 2024.

[4] M. Rossi et al., "Energy Hub and Micro-Energy Hub Architecture in Integrated Local Energy Communities: Enabling Technologies and Energy Planning Tools," Energies, vol. 17, no. 19, p. 4813, 2024.

[5] L. Ma, N. Liu, J. Zhang, and L. Wang, "Real-time rolling horizon energy management for the energy-hub-coordinated prosumer community from a cooperative perspective," IEEE Transactions on Power Systems, vol. 34, no. 2, pp. 1227-1242, 2018.

[6] A. Heidari and R. Bansal, "Probabilistic correlation of renewable energies within energy hubs for cooperative games in integrated energy markets," Electric Power Systems Research, vol. 199, p. 107397, 2021.

[7] M. Kafaei, D. Sedighizadeh, M. Sedighizadeh, and A. S. Fini, "An IGDT/Scenario based stochastic model for an energy hub considering hydrogen energy and electric vehicles: A case study of Qeshm Island, Iran," International Journal of Electrical Power & Energy Systems, vol. 135, p. 107477, 2022.

[8] A. Najafi, M. Pourakbari-Kasmaei, M. Jasinski, M. Lehtonen, and Z. Leonowicz, "A medium-term hybrid IGDT-Robust optimization model for optimal self scheduling of multi-carrier energy systems," Energy, vol. 238, p. 121661, 2022.

[9] O. Esan, N. Nwulu, and O. O. Adepoju, "A bibliometric analysis assessing the water-energy-food nexus in South Africa," Heliyon, vol. 10, no. 18, 2024.

[10] D. Rakipour and H. Barati, "Probabilistic optimization in operation of energy hub with participation of renewable energy resources and demand response," Energy, vol. 173, pp. 384-399, 2019.

[11] S. M. Moghaddas-Tafreshi, M. Jafari, S. Mohseni, and S. Kelly, "Optimal operation of an energy hub considering the uncertainty associated with the power consumption of plug-in hybrid electric vehicles using information gap decision theory," International Journal of Electrical Power & Energy Systems, vol. 112, pp. 92-108, 2019.

[12] H. Lin, Y. Liu, Q. Sun, R. Xiong, H. Li, and R. Wennersten, "The impact of electric vehicle penetration and charging patterns on the management of energy hub–A multi-agent system simulation," Applied energy, vol. 230, pp. 189-206, 2018.

[13] Y. Wang, L. Tang, Y. Yang, W. Sun, and H. Zhao, "A stochastic-robust coordinated optimization model for CCHP micro-grid considering multi-energy operation and power trading with electricity markets under uncertainties," Energy, vol. 198, p. 117273, 2020.

[14] M. M. Sani, A. Noorpoor, and M. S.-P. Motlagh, "Optimal model development of energy hub to supply water, heating and electrical demands of a cement factory," Energy, vol. 177, pp. 574-592, 2019.

[15] Y. Chen et al., "Short-term electrical load forecasting using the Support Vector Regression (SVR) model to calculate the demand response baseline for office buildings," Applied Energy, vol. 195, pp. 659-670, 2017.

[16] J. Lago, F. De Ridder, P. Vrancx, and B. De Schutter, "Forecasting Day-ahead electricity prices in Europe: The importance of considering market integration," Applied energy, vol. 211, pp. 890-903, 2018.

[17] O. Laib, M. T. Khadir, and L. Mihaylova, "Toward efficient energy systems based on natural gas consumption prediction with LSTM Recurrent Neural Networks," Energy, vol. 177, pp. 530-542, 2019.

[18] S. Atef and A. B. Eltawil, "A comparative study using deep learning and support vector regression for electricity price forecasting in smart grids," in 2019 IEEE 6th International Conference on Industrial Engineering and Applications (ICIEA), 2019: IEEE, pp. 603-607.

[19] H. Karimi, S. Jadid, and S. Hasanzadeh, "A stochastic tri-stage energy management for multi-energy systems considering electrical, thermal, and ice energy storage systems," Journal of Energy Storage, vol. 55, p. 105393, 2022.

[20] M. J. V. Pakdel, F. Sohrabi, and B. Mohammadi-Ivatloo, "Multi-objective optimization of energy and water management in networked hubs considering transactive energy," Journal of Cleaner Production, vol. 266, p. 121936, 2020.

[21] T. Liu, D. Zhang, and T. Wu, "Standardised modelling and optimisation of a system of interconnected energy hubs considering multiple energies—Electricity, gas, heating, and cooling," Energy Conversion and Management, vol. 205, p. 112410, 2020.

[22] R. Bahmani, H. Karimi, and S. Jadid, "Cooperative energy management of multi-energy hub systems considering demand response programs and ice storage," International Journal of Electrical Power & Energy Systems, vol. 130, p. 106904, 2021.

[23] S. Nojavan, K. Saberi, and K. Zare, "Risk-based performance of combined cooling, heating and power (CCHP) integrated with

renewable energies using information gap decision theory," Applied Thermal Engineering, vol. 159, p. 113875, 2019.

[24] A. S. Farsangi, S. Hadayeghparast, M. Mehdinejad, and H. Shayanfar, "A novel stochastic energy management of a microgrid with various types of distributed energy resources in presence of demand response programs," Energy, vol. 160, pp. 257-274, 2018.

[25] S. Dorahaki, A. Abdollahi, M. Rashidinejad, and M. Moghbeli, "The role of energy storage and demand response as energy democracy policies in the energy productivity of hybrid hub system considering social inconvenience cost," Journal of Energy Storage, vol. 33, p. 102022, 2021.

[26] Y. Allahvirdizadeh, S. Galvani, and H. Shayanfar, "Data clustering based probabilistic optimal scheduling of an energy hub considering risk-averse," International Journal of Electrical Power & Energy Systems, vol. 128, p. 106774, 2021.

[27] Y. Cao, Q. Wang, J. Du, S. Nojavan, K. Jermsittiparsert, and N. Ghadimi, "Optimal operation of CCHP and renewable generation-based energy hub considering environmental perspective: An epsilon constraint and fuzzy methods," Sustainable Energy, Grids and Networks, vol. 20, p. 100274, 2019.

[28] K. Cho et al., "Learning phrase representations using RNN encoder-decoder for statistical machine translation," arXiv preprint arXiv:1406.1078, 2014.

[29] J. Lee and Y. Cho, "National-scale electricity peak load forecasting: Traditional, machine learning, or hybrid model?," Energy, vol. 239, p. 122366, 2022.

[30] H. Karimi and S. Jadid, "Optimal microgrid operation scheduling by a novel hybrid multi-objective and multi-attribute decision-making framework," Energy, vol. 186, p. 115912, 2019.

[31] "https://www.kaggle.com/datasets/ernestojaguilar/shortterm-electricity-load-forecasting-panama.

Figures and Tables

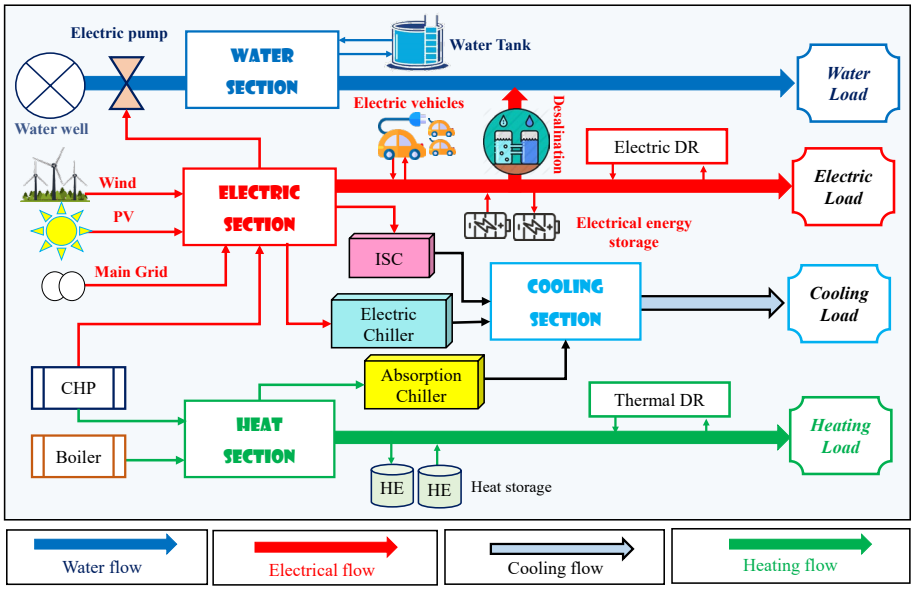

Fig. 1- Structure of proposed modern energy systems.

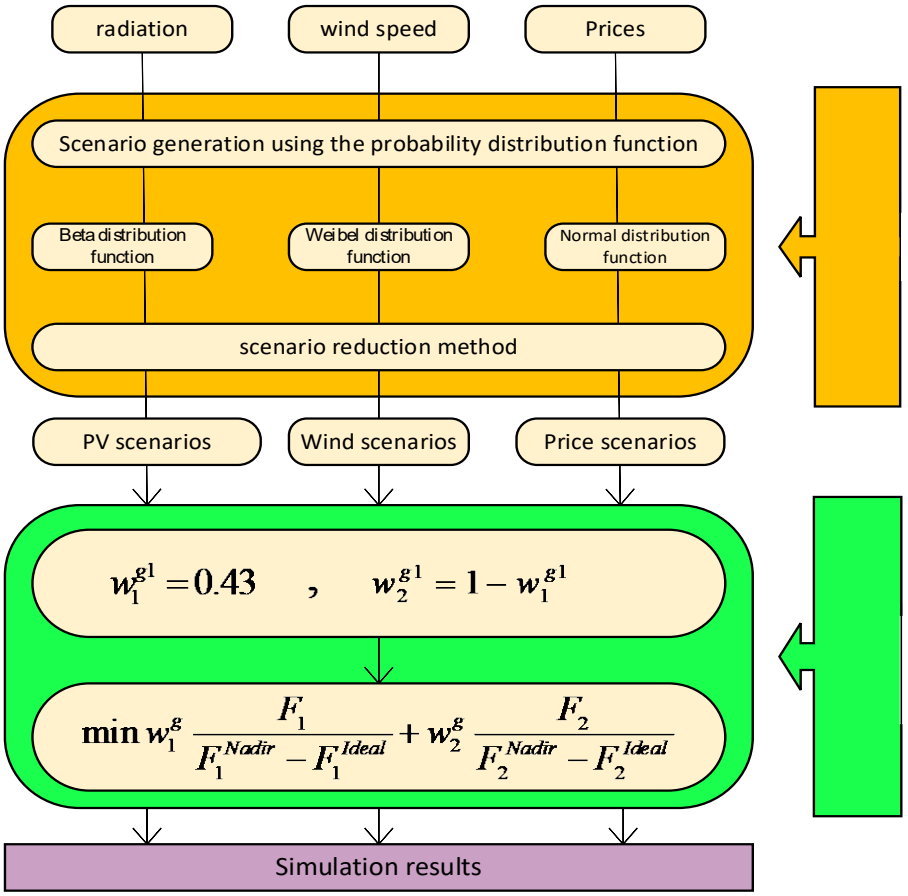

Fig. 2- Showing the simulation steps of the proposed model.

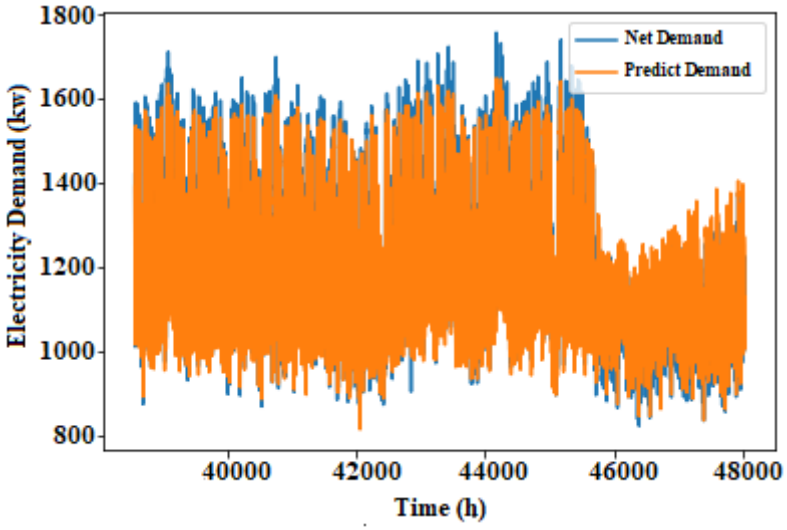

Fig. 3- Electrical load forecasting.

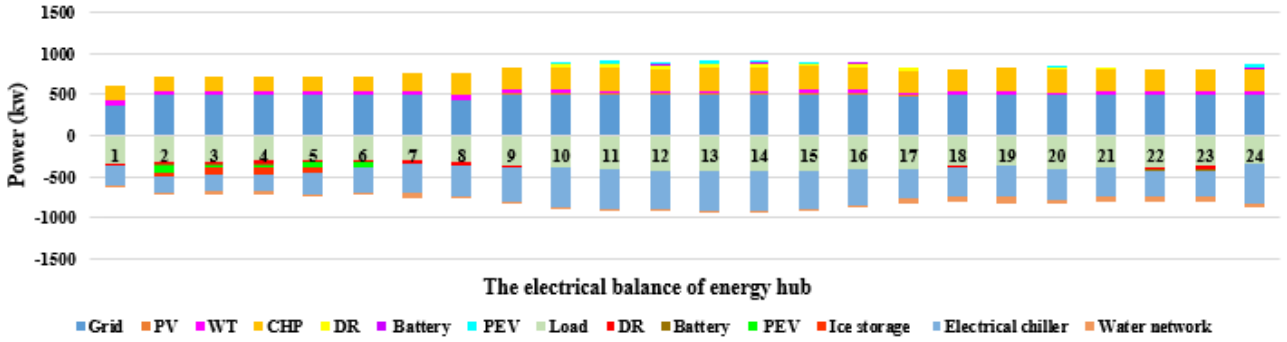

Fig. 4- The electrical balance of the system in case study 1.

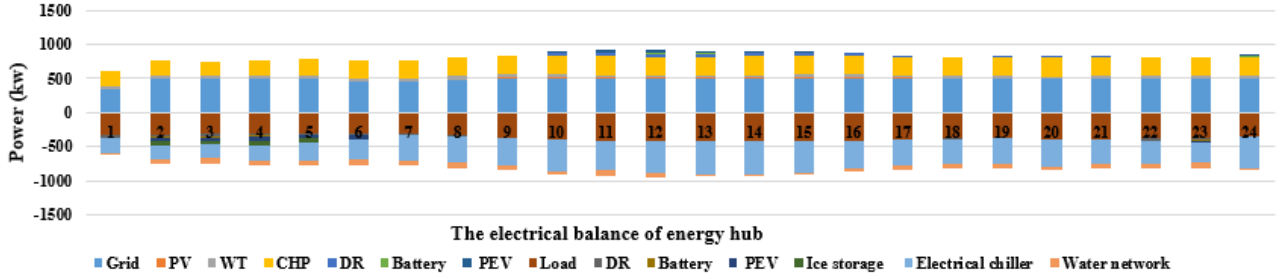

Fig. 5- The electrical balance of the system in case study 2.

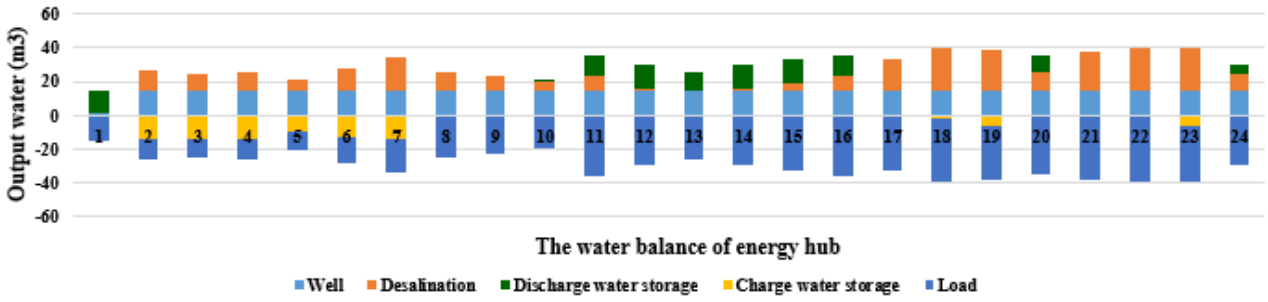

Fig. 6- The water balance of the system in case study 1.

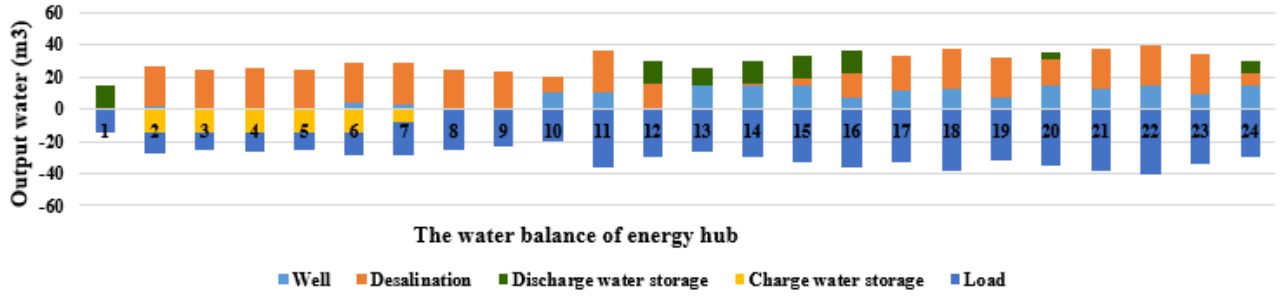

Fig. 7- The water balance of the system in case study 2.

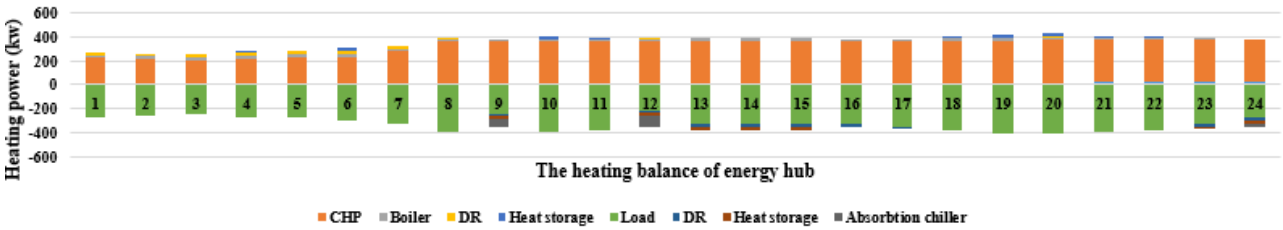

Fig. 8- The heating balance of the system in case study 1.

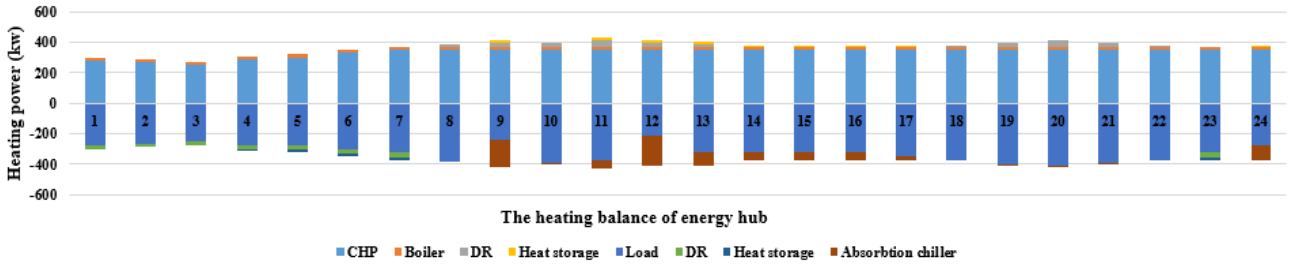

Fig. 9- The heating balance of the system in case study 2.

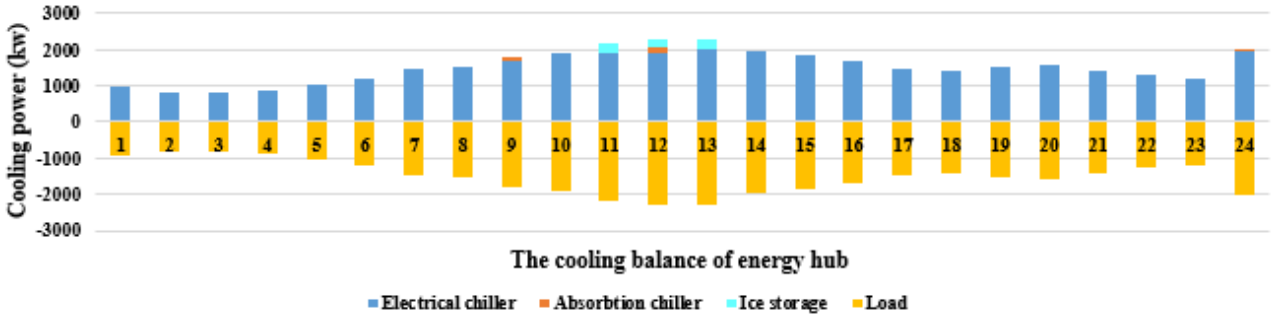

Fig. 10- The cooling balance of the system in case study 1.

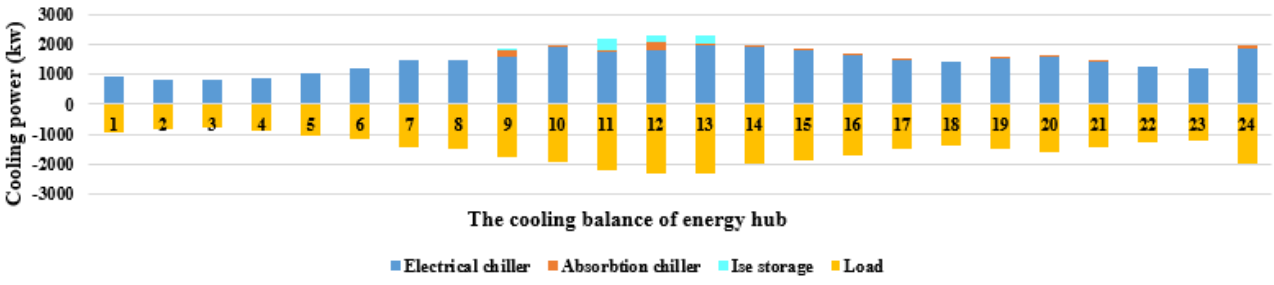

Fig. 11- The cooling balance of the system in case study 2.

Abbreviations	
AC	absorption chiller
CS	cooling storage
CHP	combined heat and power
CCHP	combined cooling, heat, and power
DR	demand response
ESS	electrical storage system
EC	electrical chiller
HS	heat storage
ISC	ice storage conditioner
IMES	integrated multi-energy system
PV	photovoltaic
RES	renewable energy resources
WT	wind turbine energy

Sets	
t	Index of time
v	Index of PEV

Parameters	
A^{pv}	PV panels area
$A^{s,w}$	water tank cross-section
B^{pv}	number of PV panel
COP^{ac}	AC performance coefficient
COP^{ec}	EC performance coefficient
COP^{isc}	ISC performance coefficient
$CR_{dr}^{e,up}$	cost of increasing electrical loads
$CR_{dr}^{e,down}$	cost of decreasing electrical loads
$CR_{dr}^{h,up}$	cost of increasing thermal loads
$CR_{dr}^{h,down}$	cost of decreasing thermal loads
C^{e,co_2}	penalty for CO2 emissions
E_{min}^{i}	minimum stored energy in storage system
E_{max}^{i}	maximum stored energy in storage system
g^{w}	gravity of earth
G_{max}^{chp}	upper bound of input natural gas to CHP
G_{max}^{boiler}	upper bound of input natural gas to boiler
H_{max}^{boiler}	upper bound of output heat to boiler
H_{max}^{ac}	upper bound of input heat to EC
I_t^{pv}	solar emission at time t
ρ^{w}	water density
λ_t^{g}	natural gas prices at time t
π_t^{e}	electricity prices
ΔD^{pev}	traveling distance
$\eta^{p,w}$	water pump efficiency
η^{pev}	efficiency of PEV
$\eta^{pev,disch}$	efficiency of PEV for discharging power
$\eta^{pev,ch}$	efficiency of PEV for charging power
$\eta^{i,ch}$	efficiency for charging mode of storage system
$\eta^{i,disch}$	efficiency for discharging mode of storage system
η^{boiler}	efficiency of the boiler
$\eta^{e,chp}$	gas-to-electricity efficiency of CHP
$\eta^{h,chp}$	gas-to-heat efficiency of CHP
$\eta^{d,w}$	water desalination energy efficiency

Variables	
$Cost^{grid}$	cost of energy trading with the grid
$Cost^{chp}$	CHP cost
$Cost^{boiler}$	boiler cost
$Cost^{emission}$	cost of pollutant CO2
$Cost^{emission}$	cost of pollutant CO2
$Cost^{EDR}$	electrical DR cost
$Cost^{HDR}$	thermal DR cost
C_t^{ec}	output power of EC
C_t^{ac}	output power of AC
ES_t^{i}	level of stored energy in energy storage i
$EE_t^{i,disch}$	binary variable for charging power
$EE_t^{i,ch}$	binary variable for discharging power
G_t^{chp}	input natural gas to CHP
G_t^{boiler}	input natural gas to boiler
H_t^{boiler}	output heat of boiler
H_t^{ac}	input heat to AC
LHV	low calorific value of natural gas
L_{max}^{grid}	upper bound of exchanged power with grid
L_t^{el}	electrical demand at time t
L_t^{wl}	water load profile
L_t^{cl}	cooling load profile
L_t^{hl}	heat load profile
$L_{max}^{s,w}$	upper bound of water tank
$LL^{w,w}$	reservoir level of water
$LL^{g,w}$	water tank height
$MRL^{i,down}$	upper bound of shifted down for DR program
$MRL^{i,up}$	upper bound of shifted up for DR program
$N^{pv,mpt}$	maximum power temperature coefficient
$P_{max}^{i,disch}$	maximum power of storage system in discharging mode
$P_{max}^{i,ch}$	maximum power of storage system in charging mode
P_{max}^{h}	maximum heat pipe power transmission
P_{wt}^{r}	rated power of WT
P_{max}^{ec}	upper bound of input power to EC
P_{max}^{isc}	upper bound of input power to ISC
$P_{max}^{pev,ch}$	upper bound of charging power of PEV
$P_{max}^{pev,disch}$	upper bound of discharging power of PEV
$P^{pev,tr}$	consumed power of PEV
$Q_{max}^{d,w}$	upper capacity of desalination unit
$Q_{max}^{w,ch}$	upper bound of charging measure of water storage
$Q_{max}^{w,disch}$	upper bound of discharging measure of water storage
$T^{pv,c}$	standard temperature
$T_t^{pv,out}$	ambient temperature at time t
SOC_{min}^{pev}	PEV minimum SOC
SOC_{max}^{pev}	PEV maximum SOC
$U_{co_2}^{grid}$	main grid CO_2 emission coefficient
U_{co2}^{boiler}	boiler CO_2 emission coefficient
$U_{co_2}^{chp}$	CHP CO2 emission coefficient for
$V_t^{ac,wt}$	wind speed
V_{wt}^{co}	cut-out speed
V_{wt}^{ci}	cut-in speed
V_{wt}^{rr}	nominal speed of WT
p_{max}^{gas}	maximum purchased gas from gas network
$II_t^{i,down}$	binary variable for down-ward DR
$II_t^{i,up}$	binary variable for up-ward DR
$L_t^{s,w}$	water level of the storage
P_t^{g}	trading power with the main grid
$P_t^{e,chp}$	electrical generation of CHP
$P_t^{h,chp}$	heat generation of CHP
$P_{t,s}^{wt}$	generating power of wind turbine
$P_{t,s}^{pv}$	output power of photovoltaic cells
P_t^{ec}	input power to EC
$PD_t^{i,down}$	down-ward power in DR program
$PD_t^{i,up}$	up-ward power in DR program
$P_t^{i,ch}$	charging power of storage system i
$P_t^{i,disch}$	discharging power of storage system i
$P_t^{pev,ch}$	PEV charging power
$P_t^{pev,disch}$	PEV discharging power
$PP_t^{pev,ch}$	PEV binary variable in charging mode
$PP_t^{pev,disch}$	PEV binary variable in discharging mode
$P_t^{pw,w}$	water well pump power consumption
$P_t^{ps,w}$	power consumption of storage pump
$P_t^{d,w}$	consumed power of water desalination
$P_t^{water,w}$	water network power consumption
P_t^{isc}	input power to ISC
P_t^{gas}	input gas from gas network
$Q_t^{w,w}$	ground water extraction
$Q_t^{d,w}$	water product of desalination unit
$Q_t^{w,ch}$	charging measure of water storage
$Q_t^{w,disch}$	discharging measure of water storage
SOC_t^{pev}	stored energy in PEV
$WW_t^{w,ch}$	status of water storage charging
$WW_t^{w,disch}$	status water storage discharging